

# Noise Bias Correction for Signal Averaged Images

E. Olariu<sup>1</sup>, A. Cardenas-Blanco<sup>2</sup>, and I. Cameron<sup>1,3</sup>

<sup>1</sup>Physics, Carleton University, Ottawa, Ontario, Canada, <sup>2</sup>Ottawa Health Research Institute, <sup>3</sup>Diagnostic Imaging, Ottawa General Hospital

## Introduction

Clinical MR images are corrupted by noise which may reduce the reliability of quantitative analyses. The extraction of the true MR signal intensity from noisy MR magnitude images is confounded by a bias, which will be referred to here as Rician Bias (RB), caused by noise rectification in the magnitude calculation for low intensity pixels<sup>1</sup>. Averaging in the image domain reduces the effective noise but not the noise bias. For low SNR a post-processing scheme to correct the noise bias<sup>2,3</sup> combined with a limited amount of signal averaging is preferable. The RB correction method discussed here, which is an implementation of the theory developed by Koay and Basser<sup>3</sup>, has been previously described<sup>2</sup>. The results are extended here to consider the effect of signal averaging and inaccuracies in the value of  $\sigma_g$  used.

## Theory

MR images are reconstructed from the magnitude of complex data. Noise on the real and imaginary signals causes a distribution of the image pixel intensities which is described by a Rician Probability Density Function (PDF)<sup>5</sup>. The mean of the Rician PDF is given by Eq. 1, where  $A$  is the pixel intensity in the absence of noise and  $I_i$  is the  $i^{\text{th}}$  order modified Bessel function of the first kind. For high SNR  $\mu_R$  is a good approximation of  $A$  but when SNR is low the difference between  $A$  and  $\mu_R$ , (i.e. the RB) is significant. Koay and Basser<sup>3</sup> have presented an analytical method based on Eq. 3 which can be used for RB correction; when accurate values for  $\mu_R$  and  $\sigma_g$  are known this gives excellent results. Unfortunately, in practice this is often not the case and approximations have to be introduced. An implementation of Koay and Basser's theory has been presented previously<sup>2</sup> which uses a binomial expansion to transform their expression into the linear correction, given by Eq. 4, to estimate the true signal  $\tilde{A}_j$  for each individual pixel. It was also suggested that the value of  $\mu_R$  in the correction term,  $\Delta\mu$ , can be calculated as an average over a small group of neighboring pixels. This approach has been shown to give very good results<sup>2</sup>. The  $\tilde{A}_j$  values, averaged over the full Rician PDF are given by Eq. 5.

Increasing the number of averages, NEX, for magnitude images causes the Rician PDF to change to a Gaussian PDF. Since the RB correction scheme used here requires reliable values for the mean of the Rician PDF, this raises the question as to whether or not the RB correction scheme works properly when NEX>1. Although the PDF shape deviates from the assumed Rician shape as NEX increases, the mean is expected to remain the same. Furthermore, the value of  $\sigma_g$  is normally determined from the mean of the background noise<sup>4</sup> using Eq. 2, which is the expression for the mean of the Rician PDF when  $A=0$ . This equation is valid for a Rician distribution but it is not clear if it applies for NEX>1, since the PDF in this case is no longer Rician.

## Methods

$N=1\times 10^6$  noisy MR signal magnitudes were generated with  $\sigma_g=1$  for given values of  $A$  and NEX and the results were displayed as histograms (bin size=0.02). The results were computed using Eq. 4 where the first term was taken to be a single pixel value averaged NEX times. In calculating the correction term,  $\Delta\mu$ , a nearest neighbor average over  $n$  pixels was used to get an estimate of  $\mu_R$ , the PDF mean. Simulations for  $n=9, 25, 100$  and  $625$  were performed for values of  $A/\sigma_g$  from 0.0 to 3.0.

## Results and Discussion

The simulation results show that the PDF shape changes from Rician to Gaussian-like as NEX increases but that the PDF mean does not change. This gives confidence that the use of Eq. 4 to correct images for RB should be valid when NEX>1. It also shows that the values of  $\sigma_g$  determined from the background of a signal averaged image are correct. This is an important result since an accurate value for  $\sigma_g$  is required in order to perform this RB correction. Fig. 1 shows several signal averaged PDFs for  $A=0$ .

Simulations were also performed as a function of the amount of error in the value of  $\sigma_g$  used. When the theoretical value of  $\mu_R$ , calculated from Eq. 1 was used for these simulations the results were found to be very insensitive to errors in  $\sigma_g$  as large as 10%. Simulations were also performed using a 9-point nearest neighbor average as an approximation of  $\mu_R$  for various amounts of error in  $\sigma_g$ . These results are shown in Table 1.

The simulations performed as a function of  $n$  and NEX showed that the RB correction improved as a function of  $nxNEX$ , converging to the correct result. For example, the same result was obtained for the 3 cases:  $n=9$ ,  $NEX=1$ ;  $n=3$ ,  $NEX=3$  and  $n=1$ ,  $NEX=9$ . This is the expected result since a nearest neighbor average over  $n$  nearest neighbors which have been signal averaged NEX times corresponds to an average over  $nxNEX$  Rician distributed values.

Signal	$\Delta\sigma=1\%$	$\Delta\sigma=3\%$	$\Delta\sigma=5\%$	$\Delta\sigma=10\%$
$A = 0.0$	1.08	2.99	4.89	10
$A = 0.2$	1.07	2.28	3.57	6.8
$A = 0.5$	0.12	2.06	3.67	1.6
$A = 1.0$	0.05	0.17	0.30	0.8
$A = 2.0$	0.01	0.03	0.03	0.05

Table 1: Sensitivity of the corrected term (% error) for various amounts of uncertainty in  $\sigma_g$  when  $A = 0.0, 0.2, 0.5, 1.0$  and  $2.0$ .

$$\mu_R = \frac{1}{2\sigma_g^2} \left\{ \exp\left(-\frac{A^2}{4\sigma_g^2}\right) \sqrt{\frac{\pi}{2}} \sigma_g \left[ (A^2 + 2\sigma_g^2) I_0\left(\frac{A^2}{4\sigma_g^2}\right) + A^2 I_1\left(\frac{A^2}{4\sigma_g^2}\right) \right] \right\} \rightarrow (1)$$

$$\mu_{R0} = \lim_{SNR \rightarrow 0} \mu_R = \sqrt{\frac{\pi}{2}} \sigma_g \rightarrow (2)$$

$$A = \sqrt{\mu_R^2 - (2-\xi)\sigma_g^2} = \sqrt{\mu_R^2 - \sigma_g^2} \rightarrow (3)$$

$$\tilde{A}_j = M_j - \mu_R \left[ \frac{1}{2} \left( \frac{q\sigma_g}{\mu_R} \right)^2 + \frac{1}{8} \left( \frac{q\sigma_g}{\mu_R} \right)^4 + \dots \right] = M_j - \Delta\mu \rightarrow (4)$$

$$\langle \tilde{A}_j \rangle_R = A = \mu_R - \Delta\mu \rightarrow (5)$$

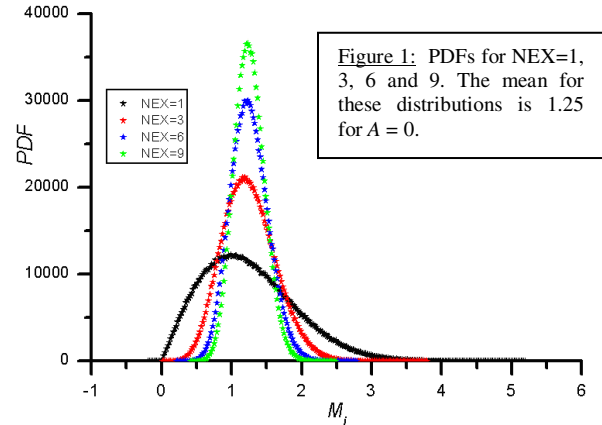


Figure 1: PDFs for NEX=1, 3, 6 and 9. The mean for these distributions is 1.25 for  $A = 0$ .

$A/\sigma_g$	Estimate of $A/\sigma_g$			
	3x3	5x5	10x10	25x25
0.0	0.257	0.214	0.161	0.108
0.2	0.286	0.249	0.208	0.180
0.5	0.433	0.428	0.450	0.492
1.0	0.902	0.958	0.992	0.999
2.0	1.986	1.996	1.998	1.999
3.0	2.996	2.999	3.000	3.000

Table 2: Distributions of the corrected term when different  $nxNEX$  and  $A/\sigma_g$  are used in the simulations.

## Conclusions

The simulation results presented here demonstrate that, even though the shape of the PDF changes as NEX increases 1) the PDF mean does not change, 2) the value of  $\sigma_g$  obtained from background signals using Eq. 3 does not change as NEX increases, 3) the RB correction technique is very insensitive to errors in  $\sigma_g$  and 4) the RB noise correction scheme gives corrected values which are consistent with the values obtained from NEX=1 images. Thus, the noise correction method used here is valid for signal averaged images.

**References:** 1) Henkelman RN, *MedPhys* 12(2) (1985); 2) Cardenas-Blanco A et al, *ISMRM*, Berlin (2007); 3) Koay CG, Basser PJ, *JMagnReson* 179 (2006); 4) Edelstein WA et al, *MedPhys* 11(1984); 5) Rice SO, *Bell Syst Technol J* 23 (1944);